Technical Note

Point Location Conversion in Distance Cartogram Construction Based on Vector Field Analysis

Takeshi Miura[1,a)] Katsubumi Tajima[1]

Received: May 13, 2020, Accepted: July 7, 2020

Abstract: Distance cartograms are deformed maps in which the distance of each of the preselected point pairs in the geographic map is changed in step with a specified value such as a travel time. In distance cartogram construction, the preselected points are fixed in the first step whereas the locations of other points are converted in the second step. This paper proposes a new point location conversion method for the second step. The conversion process is modeled as a phenomenon in a three-dimensional vector field. Each point in the geographic map is connected with the corresponding point in the cartogram by a streamline of the field. The connection relationship becomes a smooth homeomorphism required in distance cartogram construction. The experimental results demonstrate its effectiveness.

Keywords: map deformation, distance cartogram, smoothness, homeomorphism, vector field

1. Introduction

Distance cartograms are deformed maps in which the distance of each of the preselected point pairs in the geographic map is changed in step with a specified value such as a travel time [1], [2], [3]. The construction process of a distance cartogram generally consists of two steps [1], [2]. The locations of the points included in the preselected pairs such as those corresponding to train stations are fixed in the first step, whereas the locations of other points such as those comprising railroads are converted in the second step. In this paper, we focus on the second step. To maintain the readability of the cartogram, the conversion must be smooth (i.e., continuous and differentiable) and homeomorphic [1], [2]. Although several methods to maintain the above properties have been proposed [4], [5], their performances are still insufficient as will be shown in Section 3.

To guarantee the above properties, we propose a new point location conversion method used in the second step. We model the conversion process as a phenomenon in a three-dimensional vector field [6]. We arrange the geographic map and the cartogram in the vector field so that a point in the geographic map is connected with that in the cartogram by a streamline [6] of the field. When no zero-vector point exists in the field, there is a unique streamline passing through any point [6]. In the case that the vector field is smooth, therefore, the above point connection becomes a one-to-one onto smooth mapping. As a result, the conversion becomes a smooth homeomorphism [7].

We conducted experiments in which simple artificial mapping models and an actual geographic dataset were used. We compared the proposed method with the other three methods previously proposed. The experimental results showed that the proposed method could provide the best characteristics.

[1] Graduate School of Engineering Science, Akita University, Akita 010–8502, Japan
[a)] miura@mail.ee.akita-u.ac.jp

2. Point Location Conversion Method

This section describes the details of the point location conversion method. Suppose that the set of the points in the geographic map, $\mathrm{P}_{\mathrm{G}n}(x_{\mathrm{G}n}, y_{\mathrm{G}n})$ [*1] for $1 \le n \le N$ (N: total number of points), was already converted into the set of the corresponding points in the cartogram, $\mathrm{P}_{\mathrm{C}n}(x_{\mathrm{C}n}, y_{\mathrm{C}n})$ for $1 \le n \le N$, in the first step of the cartogram constructon process. To eliminate the influence of the scale difference between the geographic map and the cartogram, we separately standardize the coordinates of the points in the geographic map and those in the cartogram (origin: centroid of all points, mean distance from the centroid: unity) as follows:

$$x'_{\alpha n} = \frac{x_{\alpha n} - \hat{x}_\alpha}{\hat{d}_\alpha}, \quad y'_{\alpha n} = \frac{y_{\alpha n} - \hat{y}_\alpha}{\hat{d}_\alpha} \tag{1}$$

$$\hat{x}_\alpha = \frac{1}{N}\sum_{n=1}^{N} x_{\alpha n}, \quad \hat{y}_\alpha = \frac{1}{N}\sum_{n=1}^{N} y_{\alpha n},$$

$$\hat{d}_\alpha = \frac{1}{N}\sum_{n=1}^{N} \sqrt{(x_{\alpha n} - \hat{x}_\alpha)^2 + (y_{\alpha n} - \hat{y}_\alpha)^2} \quad (\alpha : \mathrm{G\ or\ C})$$

where $x'_{\alpha n}$ and $y'_{\alpha n}$ are the standardized coordinates of the point $\mathrm{P}'_{\alpha n}$ (corresponding to the non-standardized original point $\mathrm{P}_{\alpha n}$).

We arrange the geographic map and the cartogram in a three-dimensional space as shown in **Fig. 1**. The geographic map is put on the xy plane, whereas the cartogram is put on the $z = 1$ plane parallel to the xy plane. In Fig. 1, each point in the geographic map is connected by a line with the corresponding point in the cartogram. We give each connected point pair a unit vector as follows:

[*1] In this paper, the symbol x is used as the coordinate of the horizontal axis, whereas y as that of the vertical axis. This symbol assignment is contrary to that in the Japanese surveying and mapping community (x: northing, y: easting) [8]. We select the above assignment in accordance with mathematical conventions.

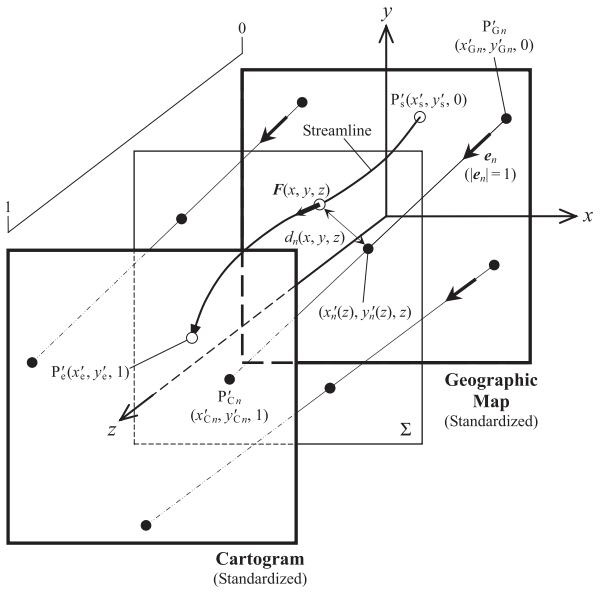

Fig. 1 Concept of vector field analysis.

$$\begin{aligned} \boldsymbol{e}_n &= \frac{x'_{Cn} - x'_{Gn}}{r'_n}\boldsymbol{i} + \frac{y'_{Cn} - y'_{Gn}}{r'_n}\boldsymbol{j} + \frac{1}{r'_n}\boldsymbol{k} \\ &= e_{nx}\boldsymbol{i} + e_{ny}\boldsymbol{j} + e_{nz}\boldsymbol{k} \qquad (2) \\ r'_n &= \sqrt{(x'_{Cn} - x'_{Gn})^2 + (y'_{Cn} - y'_{Gn})^2 + 1^2} \end{aligned}$$

where $\boldsymbol{e}_n$ is the unit vector given to the line of the nth point pair (Line $\mathrm{P}'_{Gn}\mathrm{P}'_{Cn}$, hereafter the nth line) and $\boldsymbol{i}$, $\boldsymbol{j}$ and $\boldsymbol{k}$ are the fundamental vectors for the x, y and z axes, respectively. The direction of $\boldsymbol{e}_n$ is identical to that from P'_{Gn} in the geographic map ($z = 0$) to P'_{Cn} in the cartogram ($z = 1$). Consequently, every unit vector necessarily has a positive z-component value.

We assume that the vector field $\boldsymbol{F}(x, y, z)$ shown below exists in the three-dimensional space:

$$\begin{aligned} \boldsymbol{F}(x, y, z) &= \frac{\sum_{n=1}^{N} w(d_n(x, y, z))\boldsymbol{e}_n}{\sum_{n=1}^{N} w(d_n(x, y, z))}, \quad w(d_n) = \frac{1}{d_n^q} \qquad (3) \\ d_n(x, y, z) &= \sqrt{(x'_n(z) - x)^2 + (y'_n(z) - y)^2}, \\ x'_n(z) &= x'_{Gn} + t(z)e_{nx}, \quad y'_n(z) = y'_{Gn} + t(z)e_{ny}, \quad t(z) = z/e_{nz} \end{aligned}$$

where $d_n(x, y, z)$ is the distance of the point (x, y, z) from the intersection of the nth line with the plane including (x, y, z) (Plane Σ in Fig. 1, parallel to the xy plane), $x'_n(z)$ and $y'_n(z)$ are the coordinates of the intersection and q is the parameter to adjust the strength of the weight function $w(d_n)$. $\boldsymbol{F}(x, y, z)$ is the weighted mean of $\boldsymbol{e}_n$s (with the inverse distance weight), and becomes smooth everywhere when $q > 1$ [9]. $\boldsymbol{F}(x, y, z)$ has a positive (i.e., non-zero) z-component everywhere because each of the z-components of $\boldsymbol{e}_n$s is necessarily positive.

As a result, only one streamline of $\boldsymbol{F}(x, y, z)$ passes through any point in the three-dimensional space [*2], and each streamline necessarily connects any point in the geographic map (e.g., P'_s in Fig. 1) with only one point in the cartogram (e.g., P'_e in Fig. 1) [*3].

[*2] For a smooth vector field in which no zero-vector point exists, there is only one streamline passing through any point [6].

[*3] This is caused because the z-component of $\boldsymbol{F}$ is positive everywhere. This means that streamlines of $\boldsymbol{F}$ never turn into the negative z-direction. Therefore, both the geographic map and the cartogram are intersected by a streamline only once.

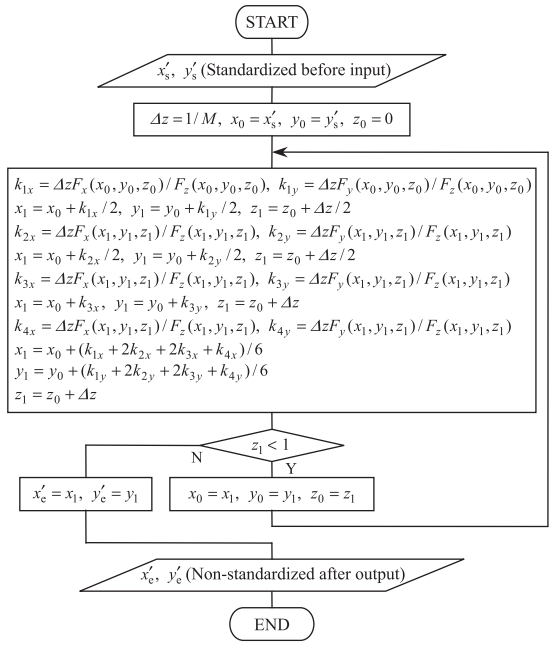

Fig. 2 Algorithm for streamline tracing (Runge-Kutta method, M: division number of the interval [0, 1] in the z axis).

Each of the points in the cartogram is also connected with only one point in the geographic map. The above connection can be regarded as a one-to-one onto mapping $f : G \to C$ (G: set of all points in the geographic map and C: set of all points in the cartogram). When $q > 1$, both f and f^{-1} are continuous and differentiable because $\boldsymbol{F}(x, y, z)$ is smooth everywhere. Consequently, f becomes a smooth homeomorphism [*4].

We adopt the above homeomorphism as a point location conversion method. A streamline of $\boldsymbol{F}(x, y, z)$ is obtained by giving a starting point and solving the equation shown below [6]:

$$\frac{dx}{F_x(x, y, z)} = \frac{dy}{F_y(x, y, z)} = \frac{dz}{F_z(x, y, z)} \qquad (4)$$

where $F_x(x, y, z)$, $F_y(x, y, z)$ and $F_z(x, y, z)$ are the x-, y- and z-components of $\boldsymbol{F}(x, y, z)$, respectively. From Eq. (4), two differential equations are derived as follows:

$$\frac{dx}{dz} = \frac{F_x(x, y, z)}{F_z(x, y, z)}, \quad \frac{dy}{dz} = \frac{F_y(x, y, z)}{F_z(x, y, z)} \qquad (5)$$

We numerically solve Eq. (5). First, the standardized point location in the geographic map, $\mathrm{P}'_s(x'_s, y'_s, 0)$, is input as a starting point ($x'_s = (x_s - \hat{x}_G)/\hat{d}_G$ and $y'_s = (y_s - \hat{y}_G)/\hat{d}_G$, x_s and y_s are the non-standardized original coordinates). This point is the point to be converted into that in the cartogram. Next, the algorithm shown in **Fig. 2** (Runge-Kutta method [10]) is executed. The execution is completed when the streamline reaches the $z = 1$ plane. Finally, the x- and y-coordinates at the intersection of the $z = 1$ plane with the streamline, x'_e and y'_e, are output. These values are converted into the non-standardized coordinates in the cartogram ($x_e = x'_e\hat{d}_C + \hat{x}_C$ and $y_e = y'_e\hat{d}_C + \hat{y}_C$).

As for the computational complexity of the above algorithm, that of the calculation of $\boldsymbol{F}(x, y, z)$, i.e., Eq. (3), is $O(N)$. On the other hand, the number of loop processing in Fig. 2 depends only

[*4] The conditions to be satisfied in a homeomorphism are as follows. (1) f is a one-to-one onto mapping and (2) f and f^{-1} are continuous [7].

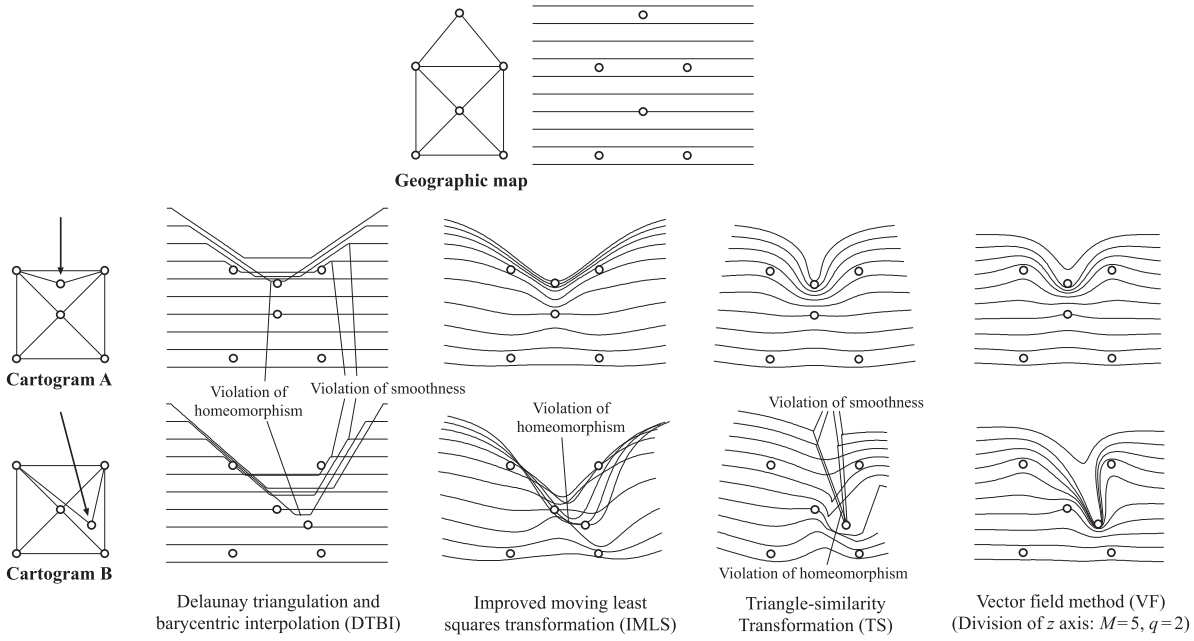

Fig. 3 Cartogram construction for simple artificial mapping models.

on the division number of the interval [0, 1] in the z axis, M [*5]. This means that this number is given independently of the parameters of the geographic map and the cartogram. As a result, the computational complexity of the whole algorithm becomes $O(N)$.

3. Results

This section presents the experimental results of the proposed vector field (VF) method. First, simple artificial mapping models are used to compare the performance of the VF method with those of the following three methods previously proposed: the combination of the Delaunay triangulation and barycentric interpolation (DTBI) [2], the improved moving least squares transformation (IMLS) [4] and the triangle-similarity transformation (TS) [5]. Next, the map of the six prefectures of the northeastern area of Japan is used to evaluate the characteristics of the VF method.

Figure 3 shows the results of the artificial mapping models. The geographic map consists of 6 points and 10 regular-interval parallel lines (150 points per line, total 1,500 points), and is converted into two cartograms: Cartograms A and B. The locations of the 6 points in the cartograms are fixed in advance (i.e., regarded as already fixed in the first step of the cartogram construction process), and the 10 lines are then converted into those in each cartogram by the VF method or the other methods. In both A and B, the point located at the highest position in the geographic map is moved downward (B is more highly deformed than A).

In the cases that the methods other than the VF method are used, the violation of homeomorphism is seen in all the cases of B. In the cases of DTBI and TS, the violation of smoothness is also seen in B. DTBI shows the violation of both smoothness and homeomorphism even in A. On the other hand, in the cases that the VF method is used (division number of the z axis: $M = 5$ and the parameter in the weight function: $q = 2$), both A and B show no violation of smooth homeomorphism.

Table 1 Numbers of smooth-homeomorphism violations.

	Cartogram	DTBI	IMLS	TS	VF
Non-differentialble point	A	16	0	0	0
(Smoothness)	B	16	0	12	0
Intersection of lines	A	8	0	0	0
(Homeomorphism)	B	26	34	18	0

The above results are summarized in **Table 1**. Specifically, the numbers of non-differentiable points represent the violation of smoothness, whereas the numbers of intersections of the 10 lines represent the violation of homeomorphism. As shown in Table 1, DTBI shows the worst characteristics (total number of smooth-homeomorphism violations: largest). Although DTBI is a commonly used method for the second step of the distance cartogram construction process, its performance is insufficient for maintaining the smooth homeomorphism. On the other hand, both IMLS and TS are better than DTBI as a whole. No violation of smooth homeomorphism in A is seen in both cases. However, the violation of homeomorphism in B is caused in both cases (IMLS is even worse than DTBI), and that of smoothness is caused in TS depending on the degree of deformation. As for the VF method, there is no violation of smooth homeomorphism in both A and B. The above tendencies suggest that the VF method is extremely robust against a highly deformed point location conversion, compared with the other methods.

Figure 4 shows the results of cartogram construction for the six prefectures of the northeastern area of Japan. The geographic map consists of 17 points, a railroad network and boundaries between prefectures. The locations of the 17 points in the cartogram are fixed in advance by analyzing the travel-time dataset of Ref. [11] [*6]. On the other hand, the locations of the points in-

[*5] We set $M = 5$ through preliminary trial-and-error experiments.

[*6] The travel-time dataset shown in Fig. 5 of Ref. [11] is used. The locations of the 17 points in the cartogram are fixed by applying the method of Ref. [3] to the above dataset. The obtained point-location configuration is identical to that used in Ref. [5].

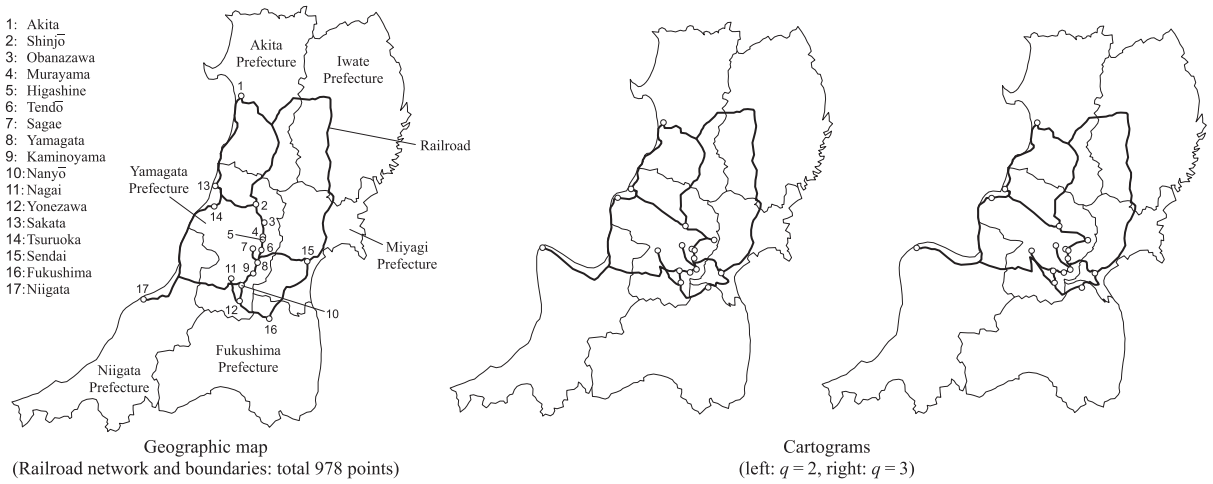

Fig. 4 Cartogram construction for the six prefectures of the northeastern area of Japan.

cluded in the railroad network and the boundaries between prefectures (978 points) are converted by the VF method. In Fig. 4, two cartograms differing in the value of the parameter q are shown (division number of the z axis: $M = 5$ in both cases). The smooth homeomorphism is realized in both cases. On the other hand, the shapes of the two cartograms are different, even though the same 17-point configuration is given. This means that users can adjust the shape of a cartogram to a certain extent by changing the q value.

The calculation time is 297 ms for both the $q = 2$ and $q = 3$ cases (CPU: Intel Core i3-350M). From the above results, we can estimate that the calculation time falls within a range of a few dozen seconds even when the data size is about 100 times that of the present cases, because the computational complexity of the VF method is $O(N)$ as already mentioned in Section 2.

4. Conclusion

The main contribution of this paper is that the proposed VF method realizes a smooth homeomorphism in the second step of distance cartogram construction. The experimental results show the robustness of the VF method against a highly deformed configuration in a cartogram. This report also suggests the adjustability of the proposed method to obtain a cartogram with a more preferable shape. To clarify the application range of the proposed method will be the subject of future work.

Acknowledgments This study was supported by JSPS Grants-in-Aid for Scientific Research (KAKENHI) Grant Number JP18K11981.

References

[1] Ullah, R. and Kraak, M.-J.: An Alternative Method to Constructing Time Cartograms for the Visual Representation of Scheduled Movement Data, *Journal of Maps*, Vol.11, No.4, pp.674–687 (2015).
[2] Bies, S. and van Kreveld, M.: Time-Space Maps from Triangulations, Didimo, W. and Patrignani, M. (Eds.), *GD 2012*, LNCS 7704, pp.511–516 (2013).
[3] Shimizu, E. and Inoue, R.: A New Algorithm for Distance Cartogram Construction, *International Journal of Geographical Information Science*, Vol.23, No.11, pp.1453–1470 (2009).
[4] Miura, T. and Tajima, K.: Improvement of Moving Least Squares Transformation in Distance Cartogram Construction, *IEEJ Trans. Electrical and Electronic Engineering*, Vol.14, pp.1879–1880 (2019).
[5] Miura, T. and Tajima, K.: Development of a Point Location Conversion Approach for Distance Cartogram Construction, *Journal of Information Processing*, Vol.28, pp.87–90 (2020).
[6] McLeod, Jr., E.B.: *Introduction to Fluid Dynamics*, Dover Publications, Inc. (2016).
[7] Zomorodian, A.J.: *Topology for Computing*, Cambridge University Press (2005).
[8] Okazawa, H., Kubodera, T., Sasada, K., Tasumi, M., Hosokawa, Y., Matsuo, E. and Mihara, M.: *Newer Surveying: Fundamentals and Applications with Newest Technology*, Corona Publishing Co., Ltd. (2014) (in Japanese).
[9] Shepard, D.: A Two-dimensional Interpolation Function for Irregularly-spaced Data, *Proc. 1968 23rd ACM National Conference*, pp.517–524 (1968).
[10] Sewell, G.: *The Numerical Solutions of Ordinary and Partial Differential Equations*, Academic Press, Inc. (1988).
[11] Kotoh, H.: Visualization of Time-Distance Network and Analysis of Regional Structures - The Multi-City Structure of Tohoku Region, *Annual Review of Tohoku University of Art and Design*, No.3, pp.94–103 (1996) (in Japanese).

Takeshi Miura received his D.Eng. degree in electrical engineering from Hokkaido University in 1998. He is currently an associate professor in the Department of Electrical-Electronic-Computer Engineering, Graduate School of Engineering Science, Akita University.

Katsubumi Tajima received his D.Eng. degree in electrical engineering from Tohoku University in 1998. He is a professor in the Cooperative Major in Life Cycle Design Engineeirng, Graduate School of Engineering Science, Akita University.